Anharmonicity of Zone-Center Optical Phonons: Raman Scattering Spectra of $GaSe_{0.5}S_{0.5}$ Layered Crystal

Physica Scripta. Vol. 65, 534–538, 2002

Anharmonicity of Zone-Center Optical Phonons: Raman Scattering Spectra of $GaSe_{0.5}S_{0.5}$ Layered Crystal

N. M. Gasanly[1,†], A. Aydinli[2,‡], C. Kocabaş[2] and H. Özkan[1]

[1] Physics Department, Middle East Technical University, 06531 Ankara, Turkey
[2] Physics Department, Bilkent University, 06533 Ankara, Turkey

Received June 6, 2001; revised version received December 3, 2001; accepted January 8, 2002

PACS Ref: 78.20.−e, 78.30.−j, 78.30. Hv

Abstract

The temperature dependencies (10–300 K) of the eight Raman-active mode frequencies and linewidths in $GaSe_{0.5}S_{0.5}$ layered crystal have been measured in the frequency range from 10 to 320 cm^{-1}. We observed softening and broadening of the optical phonon lines with increasing temperature. Comparison of the experimental data with the theories of the shift and broadening of the interlayer and intralayer phonon lines showed that the temperature dependencies can be explained by the contributions from thermal expansion, lattice anharmonicity and crystal disorder. The purely anharmonic contribution (phonon-phonon coupling) is found to be due to three-phonon processes. It was established that the effect of crystal disorder on the broadening of phonon lines is greater for $GaSe_{0.5}S_{0.5}$ than for binary compounds GaSe and GaS.

1. Introduction

The layered compounds GaSe and GaS form a series of $GaSe_{1-x}S_x$ mixed crystals with no restrictions on the concentration of the components: $0 \leq x \leq 1$ [1]. The phonon spectra of $GaSe_{0.5}S_{0.5}$ layered crystal have been reported previously at room temperature from Raman [2–4], Brillouin [5] and infrared [4,6] measurements. Room temperature Raman scattering spectra of $GaSe_{0.5}S_{0.5}$ crystal have been measured under pressure up to 1.4 GPa, and the pressure coefficients for the Raman-active modes are obtained [7].

The influence of anharmonic interactions on the lattice vibrations can be studied by measuring the phonon frequency and linewidth with temperature and pressure. A large number of articles about the temperature dependence of the frequency shift and the linewidth of the first-order Raman scattering in the semiconductors may be found in the literature [8–11]. They show that the Raman shift can be successfully modeled by including the effect of thermal expansion and the phonon-phonon coupling.

While much is known on the phonon spectra of $GaSe_{0.5}S_{0.5}$, temperature dependence of the phonon frequency and linewidth has not yet been studied. The aim of the present study was to measure the frequency and linewidth (full-width at half-maximum – FWHM), of optical phonons in $GaSe_{0.5}S_{0.5}$ layered crystals using Raman spectroscopy in the 10–300 K temperature range. We report softening and broadening of the optical phonon lines at the Brillouin zone center with increasing temperature as observed in some other semiconductors. Our analysis and results indicate that purely anharmonic contribution to the phonon frequency shift and line broadening are due to interaction with phonons of other branches. Moreover, we studied the effect of crystal disorder on the linewidth broadening of optical phonons.

2. Crystal symmetry and group-theoretical analysis

The $GaSe_{1-x}S_x$ mixed crystals, like binary compounds GaSe and GaS, have a layered structure. Each layer has four atomic planes with the sequence Se(S) - Ga - Ga - Se(S). Depending on the layer stacking kind, polytypes ε, β, γ, and δ are distinguished [12,13]. GaSe crystals grown from the melt by the Bridgman method present ε modification whereas GaS crystals invariably present β modification, which sometimes is also found in vapor-grown GaSe. At $x = 0.5$, the $GaSe_{1-x}S_x$ mixed crystal is a mixture of the ε- and β-polytypes [14].

The space groups of β-GaS and ε-GaSe crystals are D^4_{6h} and D^1_{3h}, respectively [2,3]. In the β- and ε-type structures the primitive hexagonal unit cell consists of four formula units from two neighboring layers (Fig. 1a). For GaS, there are 24 normal modes of vibration at the center of the Brillouin zone and these can be described by the irreducible representations of the D_{6h} point group

$$\Gamma \equiv 2A_{1g} + 2A_{2u} + 2B_{1u} + 2B_{2g} + 2E_{1g} + 2E_{1u} + 2E_{2g} + 2E_{2u}.$$

Thus, there are six Raman-active modes $(2A_{1g} + 2E_{1g} + 2E_{2g})$ and two infrared-active modes $(E_{1u} + A_{2u})$. For ε-polytype of GaSe, 24 normal modes are given by the irreducible representations of the D_{3h} point group

$$\Gamma \equiv 4A'_1 + 4A''_2 + 4E' + 4E''.$$

In this case, there are eleven Raman-active modes $(4A'_1 + 3E' + 4E'')$ and six infrared-active modes $(3A''_2 + 3E')$. One of the Raman-active $3E'$ modes $(E'^{(2)})$ and acoustic mode $E'^{(1)}$ are counterparts of one of the six Davydov doublets. The remaining ten Raman-active modes $(4A'_1 + 2E' + 4E'')$ are components of five Davydov doublets [15].

The symmetry coordinates found by Melvin projection operator method [16] were used to obtain the displacement vectors of atoms in all phonon modes of GaSe and GaS crystals. Figure 1b shows the atomic displacement vectors for Raman-active interlayer and intralayer modes. In these modes all the gallium and selenium (sulfur) atoms move either perpendicular or parallel to the layers.

3. Experimental details

$GaSe_{0.5}S_{0.5}$ single crystals were grown by Bridgman method. The analysis of X-ray diffraction data showed that they crystallize in a hexagonal unit cell with parameters:

†Corresponding Author. E-mail: nizami@metu.edu.tr
‡On leave from Physics Department, Baku State University, Baku, Azerbaijan. E-mail: aydinli@fen.bilkent.edu.tr

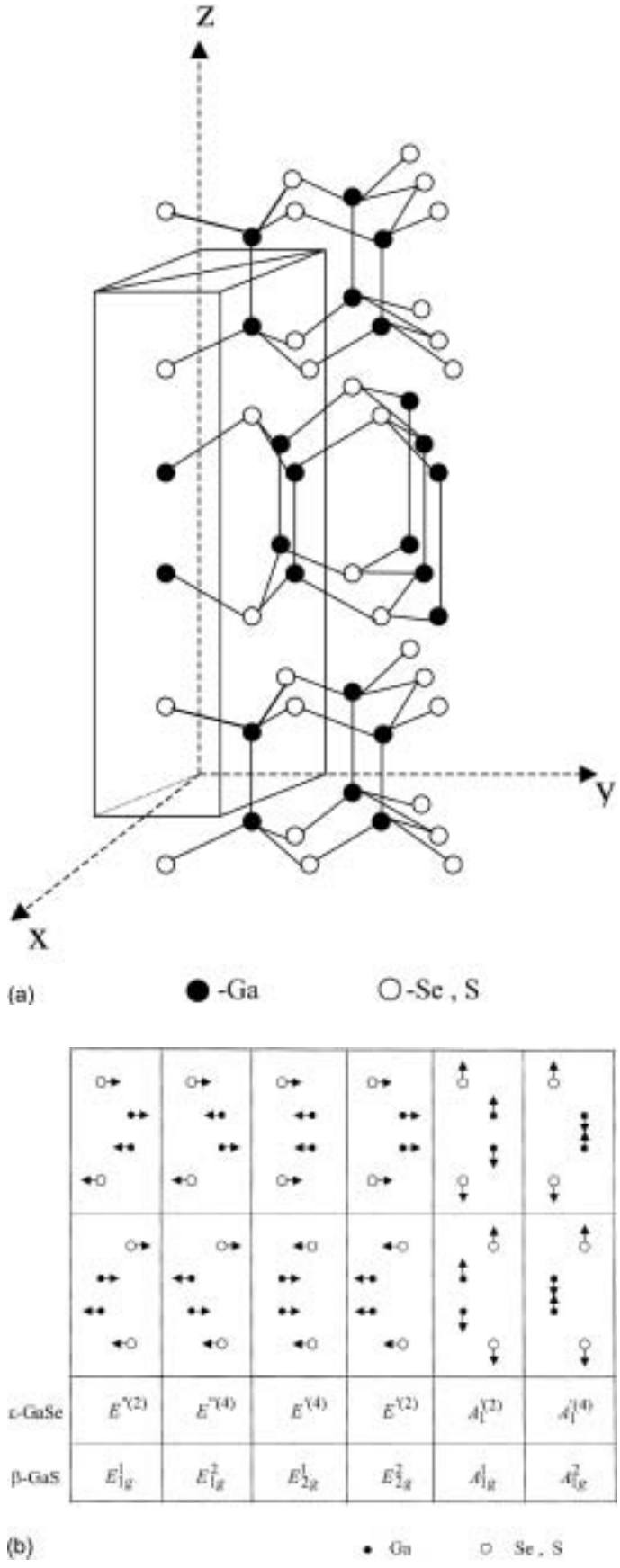

Fig. 1. (a) The unit cell of $GaSe_{0.5}S_{0.5}$ crystal. (b) Atomic displacement vectors for interlayer and intralayer Raman-active optical modes of ε-GaSe and β-GaS layered crystals.

$a = 0.3671$ and $c = 1.5719$ nm. Crystals suitable for measurements were obtained by easy cleaving perpendicular to optical c-axis.

Raman scattering measurements in $GaSe_{0.5}S_{0.5}$ layered crystal were performed in the back-scattering geometry in the frequency range 10–320 cm^{-1}. A 30 mW He-Ne laser (632.8 nm) was used as the exciting light source. The scattered light was analyzed using a "Jobin Yvon" U-1000 double grating spectrometer and a cooled GaAs photomultiplier supplied with the usual photon counting electronics. The Raman line positions were determined within an accuracy of ± 0.1 cm^{-1}. A "CTI-Cryogenics M-22" closed cycle helium cryostat was used to cool the crystals from room temperature down to 10 K. The temperature was controlled within an accuracy of ± 0.5 K. In order to avoid sample-heating effects, we have chosen a cylindrical lens to focus the incident beam on the sample.

To achieve high signal-to-noise ratio (more than 100) the slit width of the spectrometer was set to 200 μm. For slit widths below 200 μm, the signal-to-noise ratio is small so that we could not measure the linewidth of some phonon modes with high accuracy. The measured low-frequency phonon lines of $GaSe_{0.5}S_{0.5}$ crystal are so narrow that even with the indicated slit widths, one has to correct for the finite instrument resolution. The width of the response function of the spectrometer was determined by measuring the linewidth of the laser with the same slit openings as in the Raman experiment. With the slit width of 200 μm, we obtained an instrumental linewidth of 1.2 cm^{-1}. The observed peak is the convolution of the Lorentzian shape of the actual phonons with the response function of the spectrometer considered to be Gaussian. To make the deconvolution, we first fit a Voigt profile to our experimental peaks. Then we calculate the Lorentzian linewidth using the fitted width of the Voigt profile and the experimentally determined width of spectrometer response function.

4. Results and discussion

4.1. *Temperature dependence of mode frequencies*

Figure 2 represents the Raman spectra of $GaSe_{0.5}S_{0.5}$ crystal at 10 and 300 K. The shift and broadening of phonon lines with increasing temperature are seen. The present assignment of the observed modes is in agreement with that of Ref. [2,4].

Figure 3 shows the decomposition of the Raman spectra at the frequencies corresponding to the intralayer $A_1^{\prime(2)}(A_{1g}^1)$ compressional modes which have four distinct

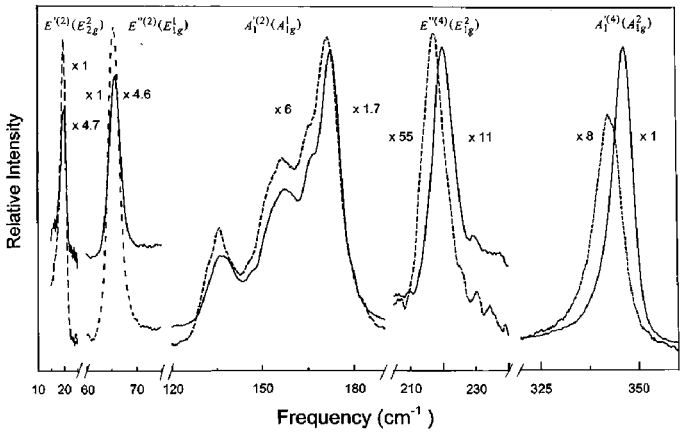

Fig. 2. Comparison of the extended individual parts of Raman spectra of $GaSe_{0.5}S_{0.5}$ crystal at $T = 10$ K (solid curves) and $T = 300$ K (dashed curves).

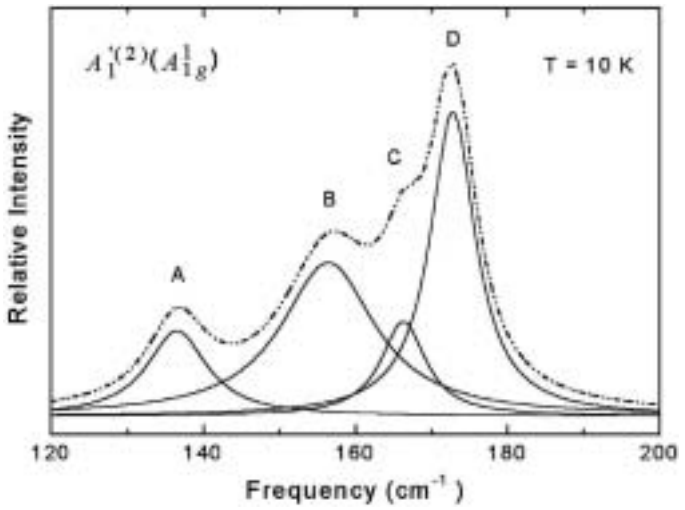

Fig. 3. The decomposition of the complex structure of the Raman-active $A_1^{\prime(2)}(A_{1g}^1)$ mode (dotted line) of $GaSe_{0.5}S_{0.5}$ crystal into components.

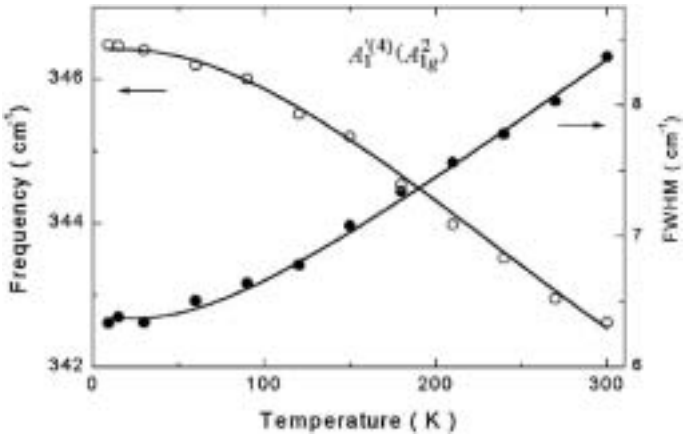

Fig. 4. Temperature dependencies of the intralayer $A_1^{\prime(4)}(A_{1g}^2)$ mode frequency (open circles) and linewidth (solid circles) in $GaSe_{0.5}S_{0.5}$ crystal. The solid curves, frequency and FWHM, give the theoretical fits using Eqs (1)–(3) for frequency and Eq. (4) for FWHM.

lines. Two lines (A and D) are genetically related to the stretching vibration of atoms in the binary crystals GaSe and GaS, respectively, while the other two lines (B and C) have frequencies intermediate to A and D lines. Therefore, in $GaSe_{0.5}S_{0.5}$ mixed crystal this stretching vibration of atoms shows a four-mode behavior depending mainly on the Ga-Ga force constant (Fig. 1). This observation is in accordance with that of Ref. [2–4].

The room temperature frequency values of $GaSe_{0.5}S_{0.5}$ mixed crystal were found to be 19.4 $[E^{\prime(2)}(E_{2g}^2)]$, 65.2 $[E^{\prime\prime(2)}(E_{1g}^1)]$, 217.0 $[E^{\prime\prime(4)}(E_{1g}^2)]$, 342.6 $[A_1^{\prime(4)}(A_{1g}^2)]$, and 135.2 (A), 154.9 (B), 165.8 (C), 171.7 (D) cm^{-1} $[A_1^{\prime(2)}(A_{1g}^1)]$. The interlayer shear mode $E^{\prime(2)}(E_{2g}^2)$ is related to the weak layer-layer interaction for which entire layers vibrate rigidly out of phase with their neighbors. The low value of this mode frequency ($\nu = 19.4$ cm^{-1}) gives information about the strength of the layer-layer interaction in $GaS_{0.5}Se_{0.5}$. In our previous study [7] we established that all mode frequencies of $GaSe_{0.5}S_{0.5}$ crystal increase with pressure. There is large difference between the mode Grüneisen parameters (γ) of the interlayer shear mode $E^{\prime(2)}(E_{2g}^2)$ (21.5), the intralayer shear modes $[E^{\prime\prime(2)}(E_{1g}^1)$ (2.1); $E^{\prime\prime(4)}(E_{1g}^2)$ (2.1)], and compressional modes $[A_1^{\prime(2)}(A_{1g}^1)$ (2.4 (A), 2.9 (B), 2.8 (D)); $A_1^{\prime(4)}(A_{1g}^2)$ (1.5)]. The difference in the mode Grüneisen parameters represents the difference in the interlayer and intralayer restoring forces. The frequency shifts of $GaSe_{0.5}S_{0.5}$ Raman modes in the temperature range 10–300 K were found to be 0.5 $[E^{\prime(2)}(E_{2g}^2)]$, 0.6 $[E^{\prime\prime(2)}(E_{1g}^1)]$, 3.1 $[E^{\prime\prime(4)}(E_{1g}^2)]$, 1.3 (A), 1.4 (B), 1.2 (D) $[A_1^{\prime(2)}(A_{1g}^1)]$ and 3.9 $[A_1^{\prime(4)}(A_{1g}^2)]$ cm^{-1}. The temperature dependencies of the frequency shift and broadening for the C line of $A_1^{\prime(2)}(A_{1g}^1)$ the mode were not analyzed due to the low intensity of its Raman scattering and the lack of Grüneisen parameter.

Analysis of the temperature dependence of the frequency shift for the low-frequency interlayer mode $E^{\prime(2)}(E_{2g}^2)$ does not yield a physically meaningful decay channel. This is consistent with the narrow linewidth of this mode which indicates a long lifetime. Figure 4 shows the experimental results (open circles) for the line positions $\nu(T)$ of one of the intralayer modes, $[A_1^{\prime(4)}(A_{1g}^2)]$. The phonon frequency shift with temperature can be described by the expression [8,17,18]

$$\nu(T) = \nu_0 + \Delta_1(T) + \Delta_2(T), \tag{1}$$

where $\nu_0 + \Delta_2(0)$ is the Raman frequency as T approaches 0 K, $\Delta_1(T)$ represents the volume dependence of the frequency due to the thermal expansion of the crystals and $\Delta_2(T)$ specifies the contribution of anharmonic coupling to phonons of other branches. $\Delta_1(T)$ can be written as

$$\Delta_1(T) = \nu_0\left[\exp\left(-3\gamma\int_0^T \alpha(T')\mathrm{d}T'\right) - 1\right], \tag{2}$$

where $\alpha(T)$ is the coefficient of linear thermal expansion.

The purely anharmonic contribution to the frequency shift can be modeled as

$$\Delta_2(T) = A\left[1 + \frac{1}{e^{x_1} - 1} + \frac{1}{e^{x_2} - 1}\right], \tag{3}$$

which represents the optical phonon coupling to two different phonons (three-phonon processes). Here, $x_1 = hc\nu_1/k_BT$ and $x_2 = hc\nu_2/k_BT$. In the present study the experiments were carried out at temperatures below the Debye temperatures of GaSe and GaS crystals ($\theta_D = 342$ [19] and 425 K [20], respectively). Thus, the three-phonon process is dominant and the higher order processes can be neglected.

The frequency shifts for intralayer modes of $GaSe_{0.5}S_{0.5}$ crystal were fitted by means of Eqs (1)–(3) using the experimental values of γ [7] and the average values of $\alpha(T)$ for GaSe [21] and GaS [21,22] with A, ν_0, ν_1, and ν_2 as adjustable parameters, keeping the sum, $\nu_1 + \nu_2 = \nu_0$, a constant (energy conservation). For all intralayer modes, the agreement between the theoretical and experimental dependencies was found to be good. Figure 4 shows this agreement for the intralayer mode $A_1^{\prime(4)}(A_{1g}^2)$. The resulting parameters for all the intralayer modes are shown in Table I.

We have also calculated separately the thermal-expansion contribution $[\Delta_1(T)]$ from Eq. (2) and the purely anharmonic contribution $[\Delta_2(T)]$ from Eq. (3) to the line shift for intralayer modes of $GaSe_{0.5}S_{0.5}$ mixed crystal by using the experimental values of $\gamma, \alpha(T)$, and the value of

Table I. *Parameters for fitting the temperature dependencies of Raman frequency and linewidth of* $GaSe_{0.5}S_{0.5}$ *crystal.*

Modes	v_0 (cm^{-1})	v_1 (cm^{-1})	v_2 (cm^{-1})	A (cm^{-1})	C (cm^{-1})	Γ_0 (cm^{-1})	Γ_0 (cm^{-1}) GaSe [29]
$E''^{(2)}(E^1_{1g})$	65.7	43.8	21.9	−0.003	0.018	1.8	–
$A_1'^{(2)}(A^1_{1g})$ (A)	136.3	91.0	45.3	0.055	0.200	9.9	0.33
$A_1'^{(2)}(A^1_{1g})$ (B)	156.0	104.0	52.0	0.176	0.332	14.4	–
$A_1'^{(2)}(A^1_{1g})$ (D)	172.5	115.0	57.5	0.315	0.349	6.5	–
$E''^{(4)}(E^2_{1g})$	220.1	146.7	73.4	−0.217	0.305	6.9	0.11
$A_1'^{(4)}(A^2_{1g})$	347.1	231.0	116.1	−0.649	1.082	5.3	0.46

adjusted parameters A, v_0, v_1 and v_2 obtained above. For the modes with Grüneisen parameter varying from 1.5 to 2.1 both contributions $\Delta_1(T)$ and $\Delta_2(T)$ are negative. For the modes having γ in the range of 2.4–2.9, $\Delta_1(T)$ continues to be negative, but $\Delta_2(T)$ changes sign and becomes positive. The variations of $\Delta_1(T)$ (dotted curves) and $\Delta_2(T)$ (dashed curves) are given in Fig. 5 for the $A_1'^{(4)}(A^2_{1g})$ and $A_1'^{(2)}(A^1_{1g})$ (line D) intralayer modes together with the experimental frequency shifts (solid curves). An interesting feature of these plots is that for $A_1'^{(4)}(A^2_{1g})$ mode with low value of Grüneisen parameter ($\gamma = 1.5$), the pure-volume contribution $\Delta_1(T)$ prevails the purely anharmonic contribution $\Delta_2(T)$, both being negative. However, for the $A_1'^{(2)}(A^1_{1g})$ mode with higher value of Grüneisen parameter ($\gamma = 2.9$), $\Delta_1(T)$ and $\Delta_2(T)$ have opposite signs. This may be associated with the difference in sets of atomic displacements for these modes. In the $A_1'^{(4)}(A^2_{1g})$ mode the restoring forces are due to the strong intralayer gallium–gallium ($C_{Ga-Ga} = 108$ and $C_{Ga-Ga} = 110$ N/m for GaSe [23] and GaS [24], respectively) and gallium-selenium (sulfur) ($C_{Ga-Se} = 123$ and $C_{Ga-S} = 130$ N/m) and weak interlayer selenium–selenium (sulfur–sulfur) ($C_{Se-Se} = 9.2$ and $C_{S-S} = 9.5$ N/m) bonds (see Fig. 1b). On the other hand, in the $A_1'^{(2)}(A^1_{1g})$ mode gallium–selenium (sulfur) bonds are not involved in the restoring forces. Here C is the compressional force constant associated with the relative displacements of the atomic planes.

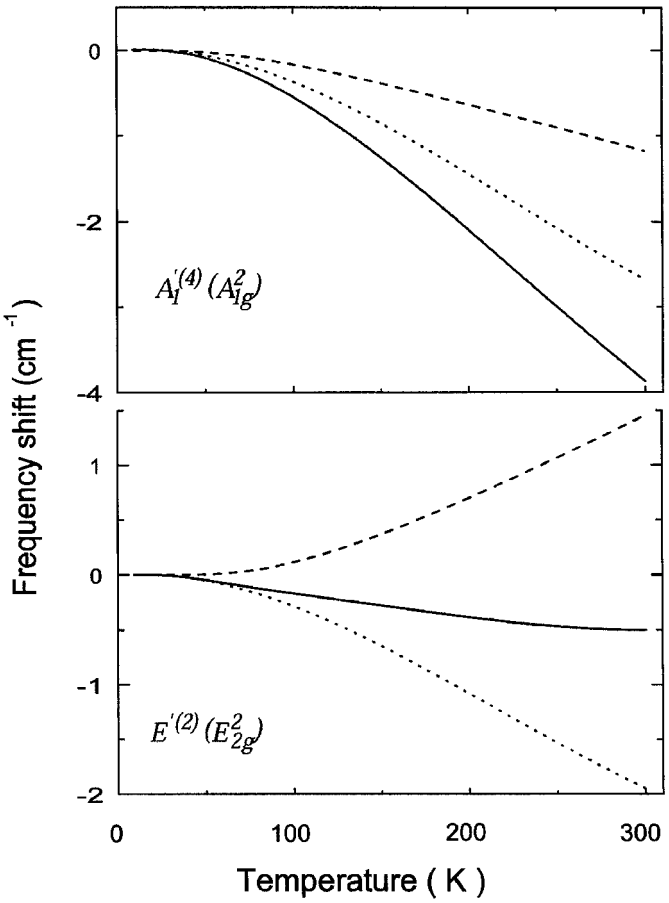

Fig. 5. Experimental Raman frequency shifts as a function of temperature (solid curves). Dotted and dashed curves are the thermal-expansion [$\Delta_1(T)$] and the purely anharmonic [$\Delta_2(T)$] contributions to the frequency shifts, respectively.

4.2. *Temperature dependence of mode linewidths*

The linewidth of the $GaSe_{0.5}S_{0.5}$ phonons was studied systematically as a function of temperature in the range of 10–300 K. The measured linewidth of interlayer mode [$E'^{(2)}(E^2_{2g})$] (1.7 cm^{-1}) at low temperatures became comparable to the instrumental linewidth (1.2 cm^{-1}). Therefore, we have not analyzed the temperature dependence of the linewidth of this mode. The corrected linewidths of intralayer Raman modes at room temperature were found to be 2.0 [$E''^{(2)}(E^1_{1g})$], 8.2 [$E''^{(4)}(E^2_{1g})$], 11.3 (A), 16.5 (B), 10.3 (C), 8.7 (D) [$A'^{(2)}(A^1_{1g})$] and 8.4 cm^{-1} [$A'^{(4)}(A^2_{1g})$]. The linewidth of all optical modes are found to increase with temperature (Fig. 2). The broadening of the phonon lines is due to anharmonicity of the lattice vibrations. The presence of anharmonic forces in a crystal lead to interactions between the harmonic normal modes. These interactions produce a temperature dependent lifetime of the normal modes.

The temperature dependence of the phonon linewidth can be described as follows [8,18,25,26]

$$\Gamma = \Gamma_0 + C\left[1 + \frac{1}{e^{x_1} - 1} + \frac{1}{e^{x_2} - 1}\right], \tag{4}$$

where Γ_0 is the temperature-independent broadening due to the disorder of crystal, C is the broadening of the phonon line due to the cubic anharmonicity at absolute zero (the decrease in phonon lifetime τ due to the decay of the optical phonon into two different phonons).

Figure 4 represents the linewidth broadening for the intralayer $A_1'^{(4)}(A^2_{1g})$ mode versus temperature. The experimental data of phonon linewidth for intralayer modes of $GaSe_{0.5}S_{0.5}$ crystal (solid circles) were fitted by means of Eq. (4) with Γ_0, C, v_1, and v_2 as fitting parameters, keeping the sum of $v_1 + v_2 = v_0$ constant. We obtain quantitative agreement between calculated curve and experimental points for intralayer $A_1'^{(4)}(A^2_{1g})$ mode (Fig. 4). The fitting parameters for all the intralayer modes are listed in Table I.

We obtained a good fit to experimental data for intralayer modes with $v_1 = 2v_2$ (see Table I). For many tetrahedral

semiconductors a reasonable fit to the temperature dependence of linewidth broadening is obtained using $v_1 = 2v_2$ [8]. The existence of a dominant contribution to the linewidth broadening for $v_1 = 2v_2$ has been confirmed by *ab initio* calculations for Ge, Si [27], GaAs [28], and GaP [17], although for diamond [27], InP and AlAs [17] $v_1 = v_2$ seems to give a better approximation to the linewidth versus temperature data.

Table I also shows the values of Γ_0 obtained for the binary compound ε-GaSe [29] for comparison. On the other hand, for fitting the temperature dependence of line broadening for binary compound GaS [30] there was no need to take into account the effect of crystal disorder (i.e., $\Gamma_0 = 0$ for all measured Raman-active modes). This may be due to two factors. First, atomic radius of the covalently bonded selenium is larger than that of sulfur (0.116 vs. 0.105 nm) leading to higher probability of defect formation. Second, as is well known, GaSe can crystallize in four different polytypes (i.e., $\varepsilon, \beta, \gamma, \delta$) while GaS crystallizes in only one (i.e., β). GaSe crystals of one polytype may contain small amounts of other polytypes, resulting in mixed-polytype crystals, which should also cause higher defect concentrations. The values of Γ_0 for $GaSe_{0.5}S_{0.5}$ mixed crystal are at least an order of magnitude larger than that for the corresponding modes in GaSe, as expected.

5. Conclusions

The Raman line shift and broadening of the optical modes in $GaSe_{0.5}S_{0.5}$ crystal with temperature are well described by purely anharmonic (phonon–phonon coupling), volume (thermal expansion), and crystal disorder contributions. The cubic (three-phonon) processes with energy conservation is responsible for the purely anharmonic contributions to the softening and broadening of the intralayer phonon lines. It was shown that the effect of crystal disorder on the line broadening is greater for $GaSe_{0.5}S_{0.5}$ crystal than that for the binary compounds GaSe and GaS.

References

1. Aulich, E., Brebner, J. L. and Mooser, E., Phys. Stat. Solidi **31**, 129 (1969).
2. Mercier, A. and Voitchovsky, J. P., Solid State Commun. **14**, 757 (1974).
3. Hayek, M., Brafman, O. and Lieth, R. M. A., Phys. Rev. B **8**, 2772 (1973).
4. Gasanly, N. M., Goncharov, A. F., Melnik, N. N. and Ragimov, A. S., Phys. Status Solidi (b) **120**, 137 (1983).
5. Yamada, M., Shimuzu, H., Maegawa, S., Yamamoto, K. and Abe, K., Physica B **105**, 334 (1981).
6. Riede, V., Neumann, H., Sobotta, H. and Levy, F., Solid State Commun. **34**, 229 (1980).
7. Gasanly, N. M., Hympanova, I. and Tagirov, V. I., 1990 Acta Phys. Univ. Comen. (Bratislava) **30**, 3 (1990).
8. Menendez, J. and Cardona, M., Phys. Rev. B **29**, 2051 (1984).
9. Gonzalez, J., Moya, E. and Chervin, J. C., Phys. Rev. B **54**, 4707 (1996).
10. Balkanski, M., Wallis, R. F. and Haro, E., Phys. Rev. B **40**, 1928 (1983).
11. Verma, P., Abbi, S. C. and Jain, K. P., Phys. Rev. B **51**, 16660 (1995).
12. Kuhn, A., Chevy, A. and Chevalier, R., Phys. Stat. Solidi (a) **31**, 469 (1975).
13. Kuhn, A., Chevy, A. and Chevalier, R., Phys. Stat. Solidi (a) **36**, 181 (1976).
14. Abdullaev, G. B., Allakhverdiev, K. R., Nani, Kh. R., Salaev, E. Yu. and Tagyev, M. M., Phys. Stat. Solidi (a) **53**, 549 (1979).
15. Yoshida, H., Nakashima, S. and Mitsuishi, A., Phys. Stat. Solidi (b) **59**, 655 (1973).
16. Melvin, M. A., Rev. Mod. Phys. **28**, 18 (1956).
17. Debernardi, A., Phys. Rev. B **57**, 12847 (1998).
18. Debernardi, A., Solid State Commun. **113**, 1 (2000).
19. Jandl, S., Brebner, J. L. and Powell, B. M., Phys. Rev. B **13**, 686 (1976).
20. Powell, B. M., Jandl, S., Brebner, J. L. and Levy, F., J. Phys. C: Solid State Phys. **10**, 3039 (1977).
21. Belenkii, G. L., Suleymanov, R. A., Abdullaev, N. A. and Shteinshraiber, V. Ya., Sov. Phys.-Solid State **26**, 2142 (1984).
22. Belenkii, G. L., Abdullayeva, S. G., Solodukhin, A. V. and Suleymanov, R. A., Solid State Commun. **44**, 1613 (1982).
23. Wieting, T.J., Solid State Commun. **12**, 931 (1973).
24. Lucazeau, G., Solid State Commun. **18**, 917 (1976).
25. Debernardi, A. and Cardona, M., Physica B **263–264**, 687 (1999).
26. Anand, S., Verma, P., Jain, K. P. and Abbi, S. C., Physica B **226**, 331 (1996).
27. Debernardi, A., Baroni, S. and Molinari, E., Phys. Rev. Lett. **75**, 1819 (1995).
28. Cardona, M. and Ruf, T., Solid State Commun. **117**, 201 (2001).
29. Gasanly, N. M., Aydinli, A., Ozkan, H. and Kocabas, C., Mat. Res. Bull. **37**, 169 (2002) (accepted).
30. Gasanly, N. M., Aydinli, A., Ozkan, H. and Kocabas, C., Solid State Commun. **116**, 147 (2000).